

OPEN

SD-OCT and Adaptive Optics Imaging of Outer Retinal Tubulation

Brett J. King*, Kaitlyn A. Sapoznik[†], Ann E. Elsner[‡], Thomas J. Gast[§], Joel A. Papay^{||},
Christopher A. Clark^{**}, and Stephen A. Burns[‡]

ABSTRACT

Purpose. To investigate outer retinal tubulation (ORT) using spectral domain optical coherence tomography (SD-OCT) and an adaptive optics scanning laser ophthalmoscope (AOSLO). To document the frequency of ORT in atrophic retinal conditions and quantify ORT dimensions versus adjacent retinal layers.

Methods. SD-OCT images were reviewed for the presence of retinal atrophy, scarring, and/or exudation. The greatest width of each ORT was quantified. Inner and outer retinal thicknesses adjacent to and within the area of ORT were measured for 18 patients. AOSLO imaged ORTs in five subjects with direct and scattered light imaging.

Results. ORT was identified in 47 of 76 subjects (61.8%) and in 65 eyes via SD-OCT in a wide range of conditions and ages, and in peripapillary atrophy. ORTs appeared as finger-like projections in atrophy, seen in the *en face* images. AOSLO showed some ORTs with bright cones that guide light within atrophic areas. Multiply scattered light mode AOSLO visualized variegated lines (18–35 μm) radiating from ORTs. The ORTs' width on OCT b-scan images varied from 70 to 509 μm . The inner retina at the ORT was significantly thinner than the adjacent retina, 135 vs. 170 μm ($P = .004$), whereas the outer retina was significantly thicker, 115 vs. 80 μm ($P = .03$).

Conclusions. ORTs are quite common in eyes with retinal atrophy in various disorders. ORTs demonstrate surviving photoreceptors in tubular structures found within otherwise nonsupportive atrophic areas that lack retinal pigment epithelium and choriocapillaris.

(Optom Vis Sci 2017;94:411–422)

Key Words: outer retinal tubulation, adaptive optics scanning laser ophthalmoscope (AOSLO), photoreceptors

Typically, it is thought that the atrophy of the retinal pigmented epithelium and choroid leads to a complete loss of the overlying photoreceptors.¹ Thus, in atrophic outer retinal disorders, such as geographic atrophy, the photoreceptors are often assumed to be absent. This assumption has come into question with the recognition of outer retinal tubulation by Zweifel et al.² Outer retinal tubulations are tubular structures that are visualized on

spectral domain optical coherence tomography (SD-OCT) in single B-scans as nonedematous circular or ovoid structures at the level of the outer nuclear layer found near or overlying outer retinal atrophy. Outer retinal tubulations have a hyperreflective border with varying degrees of hyperreflectivity within their structure² (Fig. 1). Although outer retinal tubulations have been mistaken for cysts, when a series of B-scans is available, it becomes clear that outer retinal tubulations are not isolated structures, but form tubes or flattened tubes.² These tubes apparently arise from remodeling of the normal outer retina that occurs in a “rolling” mechanism² with the outer segment extending radially into the lumen of the tube. These networks of tubes differ in their cellular structure from the adjacent retinal layers, with outer retinal tubulations possibly altering the relative thicknesses of the overlying versus adjacent layers of the retina investigated in this study.

As these and similar structures have been identified in association with a large number of outer retinal degenerations and dystrophies ranging from nonexudative age-related macular degeneration to choroideremia,^{2–6} it is unlikely that outer retinal tubulation are disease-specific and instead represent a general response to retinal

*OD, FAAO

[†]OD

[‡]PhD, FAAO

[§]MD, PhD

^{||}BS

^{**}OD, PhD

School of Optometry, Indiana University, Bloomington, Indiana (all authors).

This is an open-access article distributed under the terms of the Creative Commons Attribution-Non Commercial-No Derivatives License 4.0 (CCBY-NC-ND), where it is permissible to download and share the work provided it is properly cited. The work cannot be changed in any way or used commercially without permission from the journal.

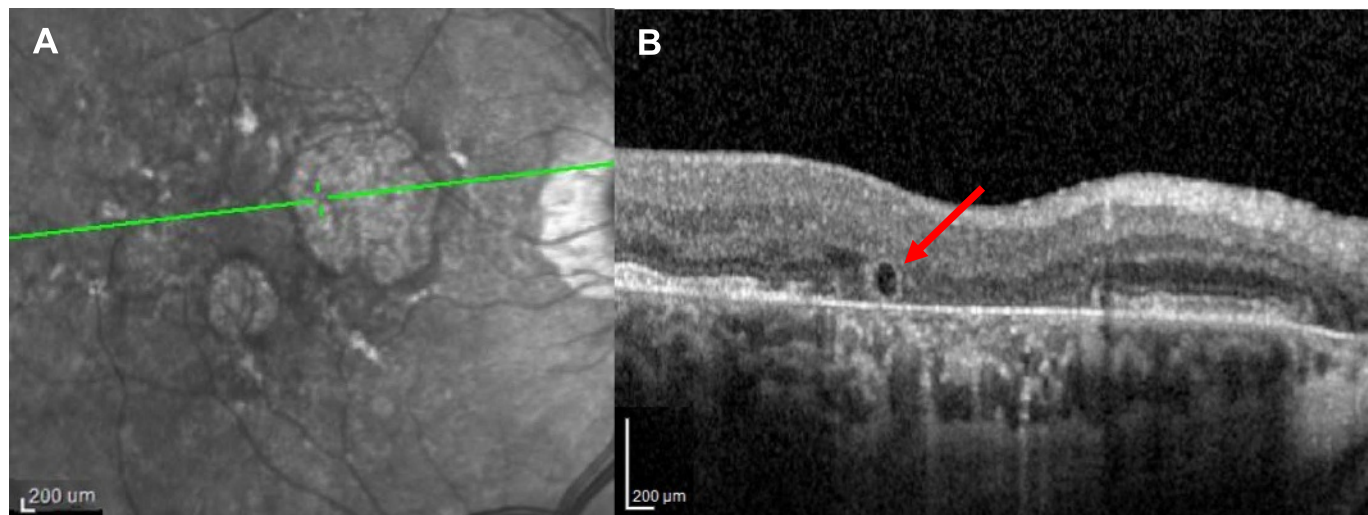


FIGURE 1.

SD-OCT imaging of an ORT in a 76-year-old subject with nonexudative AMD. (A) Infrared image showing location of the cross-sectional SD-OCT image (B) within an area of geographic atrophy. (B) SD-OCT b-scan of ORT (red arrow) with hyperreflective border adjacent to an edge of geographic atrophy.

disease. The initial identification of outer retinal tubulations on SD-OCT demonstrated a substantial proportion (24%) of patients with outer retinal tubulations in a tertiary retinal referral practice largely serving patients with age-related macular degeneration, albeit with comorbidities.² Wolff et al.⁷ found similar structures to be common in exudative age-related macular degeneration (56%) and less common in atrophic age-related macular degeneration (21%). Subsequent studies have noted the characteristics of patients and their visual outcomes while undergoing therapy for exudative age-related macular degeneration, with a substantial proportion having outer retinal tubulations (22%).⁸ Despite the large proportions of affected individuals, the clinical significance of outer retinal tubulations is unclear. Less rapid advancement of geographic atrophy in the presence of outer retinal tubulation has been reported.⁸ In contrast, other studies find faster enlargement of geographic atrophy⁹ and poorer visual acuity in eyes with outer retinal tubulations.⁸

Although SD-OCT investigations brought outer retinal tubulations to clinical attention, these structures were described with histology at least as early as 1996.¹⁰ Recently, SD-OCT findings of outer retinal tubulation have been directly compared^{11–13} and correlated¹³ to histological findings in age-related macular degeneration subjects,^{11–13} suggesting they are defined by an external limiting membrane and inner segment mitochondria.¹² The outside of an outer retinal tubulation is the border of cones in various phases of degeneration, which may still be connected to the inner retina in a 360-degree radial pattern.¹¹

Despite the cones being located in a region of retinal pigment epithelial atrophy, some functionality of the cones within outer retinal tubulations has been proposed based on perimetry data.² The radial orientation of cones and debris makes it unlikely that cones can capture light efficiently or provide a normal Stiles-Crawford effect. Functional cones within outer retinal tubulations are likely those in earlier phases of degeneration, which still possess shortened outer segments. However, the functionality of these cones is likely diminished with severely decreased visual sensitivity within areas of outer retinal tubulations.

In the current study, we provide a more complete description of outer retinal tubulations *in vivo*, combining SD-OCT and adaptive

optics scanning laser ophthalmoscope imaging.¹⁴ In particular, adaptive optics scanning laser ophthalmoscope is advantageous in imaging outer retinal tubulations as it provides high-resolution images using both confocal and multiply scattered light enabling simultaneous viewing of both cone inner and outer segments. This is advantageous as in confocal imaging there is the potential of misidentifying cones as other possible highly reflective structures that are in the same plane¹⁵ and enables cone inner segments to still be identified without functioning or absent outer segments likely to be characteristic of the cones found in outer retinal tubulations. We next used SD-OCT to quantify the dimensions of outer retinal tubulations with respect to their overlying and surrounding retina in eyes that were generally not exudative. By evaluating changes in inner and outer retinal thickness, we provide data for the assessment in the change in proximity of surviving photoreceptors to retinal vasculature that may provide some metabolic support to the cones in the absence of normal retinal pigmented epithelium and choriocapillaris. We also hypothesized that as this study was performed from an optometric referral population that is not limited to those undergoing therapy for active exudation, there would be an even greater frequency of outer retinal tubulations than in the majority of previous reports if outer retinal tubulation are a generalized response of the retina to atrophy.

METHODS

Subjects

The SD-OCT portion of this study is a retrospective study based on existing patient data, but selected subjects were studied prospectively with adaptive optics scanning laser ophthalmoscope imaging and SD-OCT. Patients with retinal atrophy were entered into the study. SD-OCT data were collected between December 2008 and January 2014. Subjects who were imaged prospectively had the nature and possible consequences of the study explained, and then signed a consent form that was approved by the Indiana University Institutional Review Board (IRB). All study protocols, including both adaptive optics scanning laser ophthalmoscope imaging and

retrospective chart reviews, were approved by the Indiana University IRB and adhered to the Declaration of Helsinki.

Patient Selection

First, a clinic database search based on diagnostic codes for presumed ocular histoplasmosis, ocular toxoplasmosis, age-related macular degeneration, hereditary retinal dystrophies, macular scarring, and hereditary choroidal dystrophies was performed. The search returned records for 489 patients. Next, patients were selected who had SD-OCT B-scans (Spectralis; Heidelberg Engineering, Heidelberg, Germany) demonstrating retinal atrophy, scarring, and/or exudation. Each available infrared SLO fundus image and retinal SD-OCT image were reviewed by two authors to determine the presence of outer retinal atrophy independently (BJK and KAS). This resulted in 80 subjects. In four of these subjects, outer retinal tubulation was found in association with solely peripapillary atrophy.

Because peripapillary atrophy is not necessarily a pathologic finding as the microenvironment and retinal thicknesses are likely to be different at these locations compared to parafoveal locations, these four subjects were excluded from further analysis leaving 76 qualified subjects. Finally, from this group of 76 subjects, 5 subjects were enrolled for additional adaptive optics scanning laser ophthalmoscope and SD-OCT imaging based on the presence of outer retinal tubulations, availability for testing, adequate fixation stability, and media clarity.

Analysis of SD-OCT Images

The records of both eyes of the 76 subjects were reviewed for the presence of outer retinal tubulation using Zweifel's criteria,² which included outer retinal round or ovoid structures with hyperreflective borders and varying degrees of internal reflectivity in OCT b-scans.² When multiple dates of images with atrophy and/or outer retinal

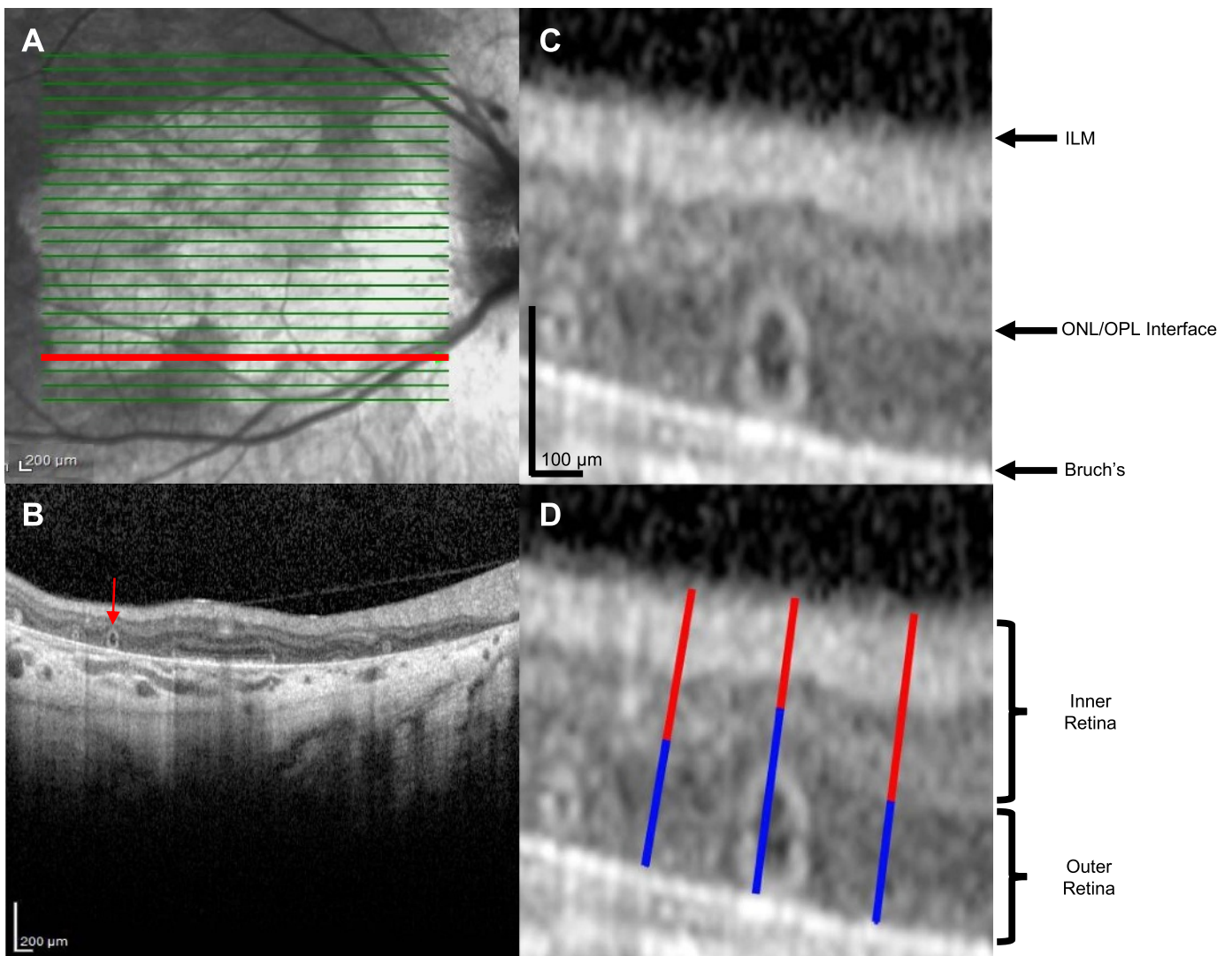


FIGURE 2.

Technique used for measuring retinal thickness and ORT cross-sectional size. (A) Example of b-scan location (red line) with ORT used for retinal thickness measurements. (B) Corresponding B scan showing numerous ORT. Red arrow indicates ORT shown in C and D in which adjacent measurements of retinal thickness were taken. (C) Enlarged image of ORT in B (red arrow) and labeled retinal layers. (D) Measurement of retinal thickness at the site of an ORT was performed for the inner retina, from ILM to the top of the outer nuclear layer (red) and from the top of the outer nuclear layer to Bruch's membrane (blue). This measurement was made directly above an ORT and adjacent to the ORT.

TABLE 1.

Patient population according to diagnosis and presence or absence of outer retinal tubulation (ORT)

	ORT	No ORT
N (subjects)	47	29
N (eyes)	65	87
Gender (proportion female)	0.55	0.41
Median age	80	81
Mean age	74.1 (± 15.5)	76.6 (± 14.7)
Primary diagnosis (N)		
Age-related macular degeneration	39	24
Central serous chorioretinopathy	1	0
Unspecified hereditary chorioretinal dystrophy	1	0
Presumed ocular histoplasmosis	1	3
Pattern dystrophy	0	1
Rod-cone dystrophy	2	0
Stargardts	1	0
Thioridazine toxicity	1	0
Ocular toxoplasmosis	1	0
Retinal pigmented epithelial detachment (scar)	0	1

tubulation were available for an eye, the most current image of acceptable quality was included in the study, and the age of the patient at the time of the image acquisition selected was determined. In the images where outer retinal tubulations were present, further analysis was performed to determine the outer retinal tubulation cross-section width. The integrity of the ellipsoid zone on the b-scans was used as a measure of photoreceptor presence. The SD-OCT images were converted to tiff files and uploaded to Photoshop CS6 (Adobe, San Jose, CA). The maximum width of each individual outer retinal tubulation cross-section was measured and the average calculated.

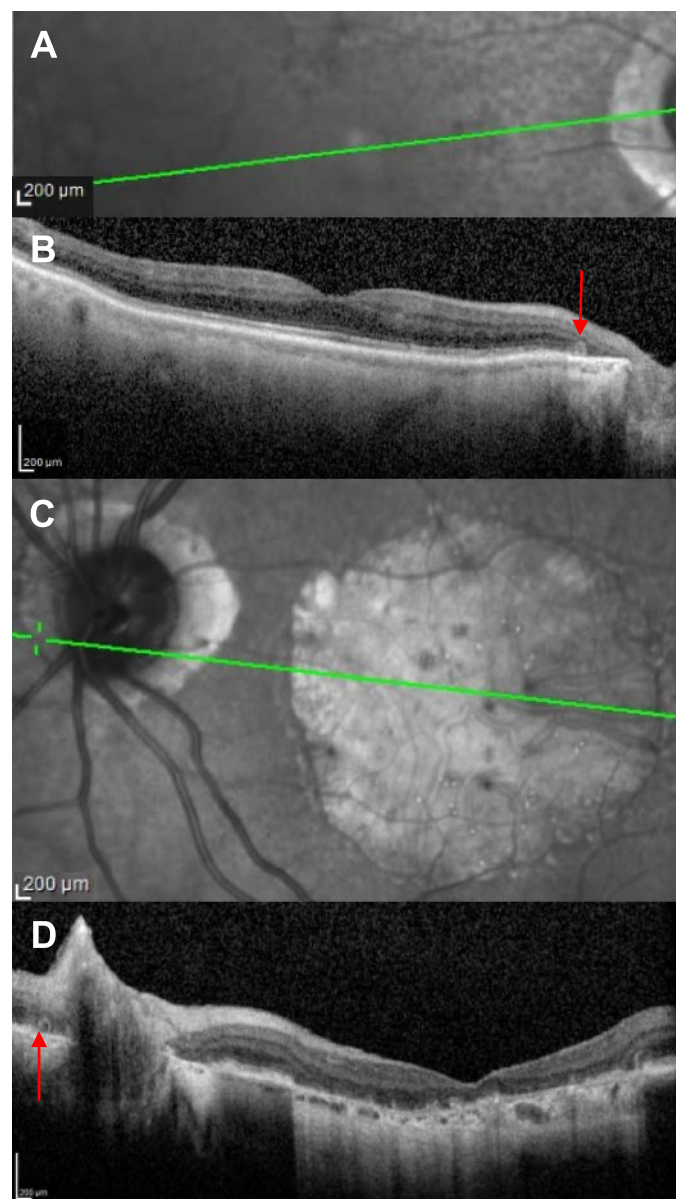
Analysis of Retinal Thickness

To examine the relation of outer retinal tubulation to inner and outer retinal thickness, we selected one eye of patients with outer retinal tubulation but without exudative disease or outer retinal tubulations in the foveal region because of the rapid variation in normal retinal thickness at this location. The inclusion criteria for thickness provided data from 18 of the 76 subjects. The best single b-scan containing a high-contrast outer retinal tubulation image from one eye of each qualified patient was then imported and quantified in Photoshop CS6 as a tiff file. Measurements of the thickness of the inner retina (top of outer nuclear layer to the inner limiting membrane) and the outer retina (from the top of the outer nuclear layer to Bruch's membrane) were obtained by manual grading (Fig. 2) for regions at and adjacent to the outer retinal tubulation. All thickness measurements were made orthogonally to the retinal surface. Measurements adjacent to the outer retinal tubulation were made where the top of the outer nuclear layer dipped back to near normal position (Fig. 2).

Adaptive Optics Scanning Laser Ophthalmoscope Imaging

In vivo adaptive optics scanning laser ophthalmoscope imaging of the outer retinal tubulation structure and photoreceptor status

in the adjacent environment was performed on a subset of five patients with retinal degenerations, including rod-cone dystrophy and age-related macular degeneration. Patients who returned for adaptive optics scanning laser ophthalmoscope imaging received a retinal examination, including indirect ophthalmoscopy, and a high-density macular SD-OCT scan, with B-scan spacing of 60 μm or less (Spectralis; Heidelberg Engineering, Heidelberg, Germany) if they had not received one recently. Axial lengths were measured using an IOL Master (Carl Zeiss Meditec, Dublin, CA).

**FIGURE 3.**

ORT found in parapapillary atrophy (PPA) in subjects without and with other atrophic changes of the outer retina imaged by SD-OCT. (A) and (B) Infrared (IR) reflectance image with b-scan location and corresponding b-scan of an ORT (red arrow) at the edge of PPA in an 87-year-old white female patient with NEAMD. (C) and (D) IR reflectance image with b-scan location and corresponding b-scan of an ORT (red arrow) at the edge of PPA in an 87-year-old white female patient with geographic atrophy. Although not shown in the selected b-scan, this subject has other ORTs associated with her geographic atrophy.

The Indiana adaptive optics scanning laser ophthalmoscope was used to acquire *en face* retinal images with subcellular resolution, at high contrast, as previously described.^{16,17} Both confocal and multiply scattered light images of each patient's retina were taken either simultaneously or sequentially. Multiply scattered light images were obtained by displacing the aperture of one of the imaging channels.^{18,19} Imaging was performed by first focusing in regions surrounding the atrophy, near the outer retinal tubulation, and then moving to the outer retinal tubulation and along its border, as guided by the reviewed SD-OCT and *en face* images. At each retinal location, approximately 100 video frames were acquired. The scan was then steered to adjacent regions with about 50% overlap between frames. Most images were acquired with a field size of 2.0×1.8 deg. This field size produces a pixel spacing of $1 \mu\text{m}$ per pixel for a typical emmetropic eye. The magnification was increased or decreased to provide more detail of a feature or more details of the surrounding retina. The corresponding pixel spacing was decreased by 0.6, producing a 1.33×1.2 deg field size or increased by 1.66, producing a 3.3×3 deg field size. The lateral optical resolution by the Rayleigh criterion was approximately $2 \mu\text{m}$ for a fully dilated eye, although for this population full dilation to 8 mm was not always possible. In those cases, optical resolution was somewhat less, being inversely related to pupil size.

After imaging, the individual frames were corrected for sinusoidal distortion resulting from resonant galvanometer-driven scanning. The corrected individual frames were averaged using a technique to weight the best images²⁰ because in older populations, tear film dynamics can alter image quality over time. When possible, structural characteristics of the outer retinal tubulations were measured after processing. This also includes variegated structures appearing as dark and bright lines running perpendicular to the measurement beam, thus allowing for length estimates within the imaging plane from the apparent outer retinal tubulation border outward. Contrast of images was adjusted in the accompanying figures for best visualization of outer retinal tubulation characteristics.

Statistical Analysis

For the 76 qualified subjects, a *t*-test was performed to compare age differences between subjects with and without outer retinal tubulation. Statistical analyses were performed using SAS 9.4 (SAS Institute Inc., Cary, NC).

RESULTS

Of the 76 qualified subjects, 47 subjects (61.8%) possessed one or more outer retinal tubulation in at least one eye. Of the 152 eyes, 65 (42.7%) possessed one or more outer retinal tubulation. The average age of the patients with outer retinal tubulation was 74 years with a range of 22 to 96 years; outer retinal tubulations were associated with a variety of retinal disorders (Table 1). As evident from Table 1, age-related macular degeneration was the most common associated pathology and had a proportion (62%) similar to our overall proportion of patients with outer retinal tubulation; however, outer retinal tubulation appears to develop in a large variety of retinal pathologies that caused extensive atrophy of the outer retina. Additionally, outer retinal tubulation was associated with peripapillary atrophy in seven eyes (Fig. 3). Four of these eyes had no other retinal pathology, and the outer retinal tubulation was found associated solely with peripapillary atrophy. The other three eyes with outer retinal tubulations related to the peripapillary atrophy also had additional outer retinal tubulations associated with another region of retinal degeneration.

There was no statistically significant difference in age between subjects with and without outer retinal tubulation ($t = 0.70$, $P = .49$), and the distribution of the ages and number of subjects between these two groups was relatively similar (Fig. 4).

Analysis of SD-OCT b-scan images revealed that outer retinal tubulations are commonly found at the border of atrophic and less abnormal retina (Fig. 5). The photoreceptor layers, particularly

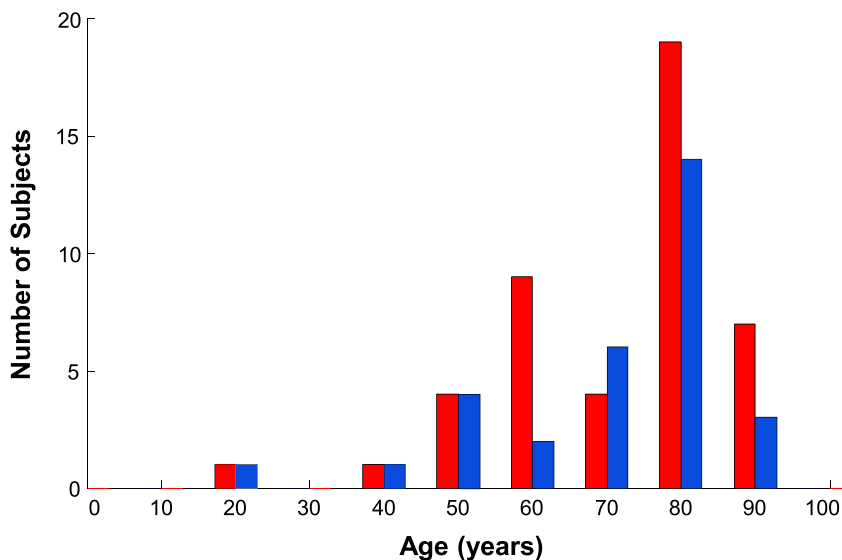


FIGURE 4.

Distribution of ages for subjects. Blue: patients with outer retinal tubulation. Red: patients with atrophy but no detected outer retinal tubulation.

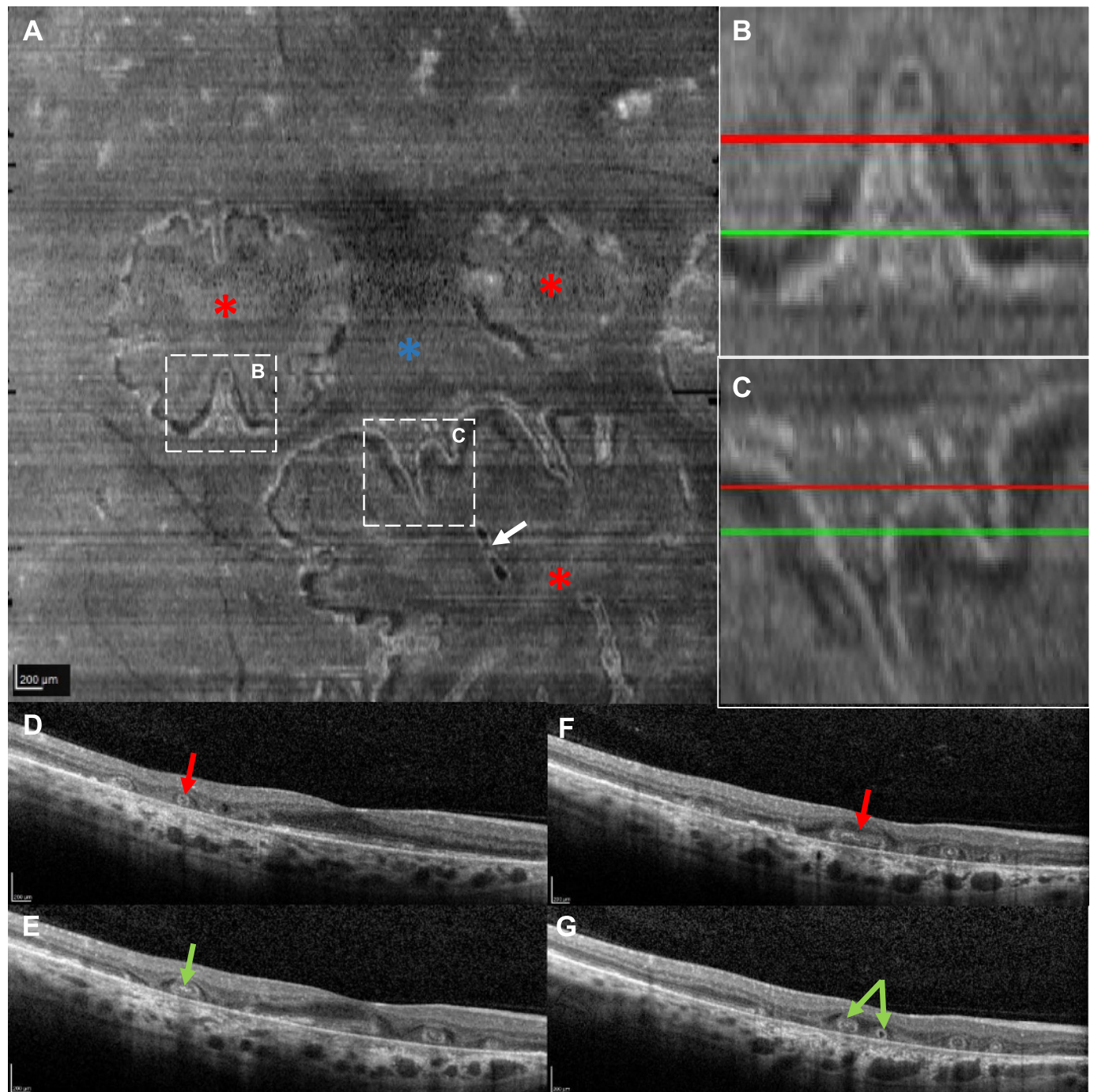


FIGURE 5.

SD-OCT imaging of ORT in a 56-year-old subject with rod-cone dystrophy demonstrating extensive networks of ORTs and large variations in their topography and width. (A) En face image showing several areas of outer retinal atrophy (red asterisks) with numerous ORT extending from more normal retinal into atrophic regions. The fovea is denoted by the blue asterisk. Note, one ORT (white arrow) is completely enclosed within an atrophic region. (B) Magnified regions of an ORT in (A) (dashed lines) showing two locations of cross-sectional images in (D) and (E). (C) Magnified region of branching ORT in (A) (long dashed lines) showing location of cross-sectional images (F and G). (D) Cross-sectional image of ORT (red arrow, cross-section location: red line in B). (E) Cross-sectional image of ORT (green arrow, cross-section location: green line in B). (B), (D), and (E) demonstrate the variation in size of a single ORT. (F) Cross-sectional image of horizontally elongated ORT (red arrow, cross-section location: red line in C). (G) Cross-sectional image of two branches (green arrows, cross-section location: green line in C) of ORT in (F). (C), (F), and (G) demonstrate an ORT that branches into two distinct ORT as it extends into an atrophic region.

the ellipsoid zone, were not apparent in areas containing outer retinal tubulations. The average OCT b-scan width for outer retinal tubulations was 165 μm with sizes ranging from 70 to 509 μm . In some patients, we were able to show changes over time in

outer retinal tubulation. Fig. 6 shows an outer retinal tubulation in one nonexudative age-related macular degeneration patient in which at time 1 there is a disruption and elevation of the myoid and ellipsoid, and 6 months later an outer retinal tubulation is

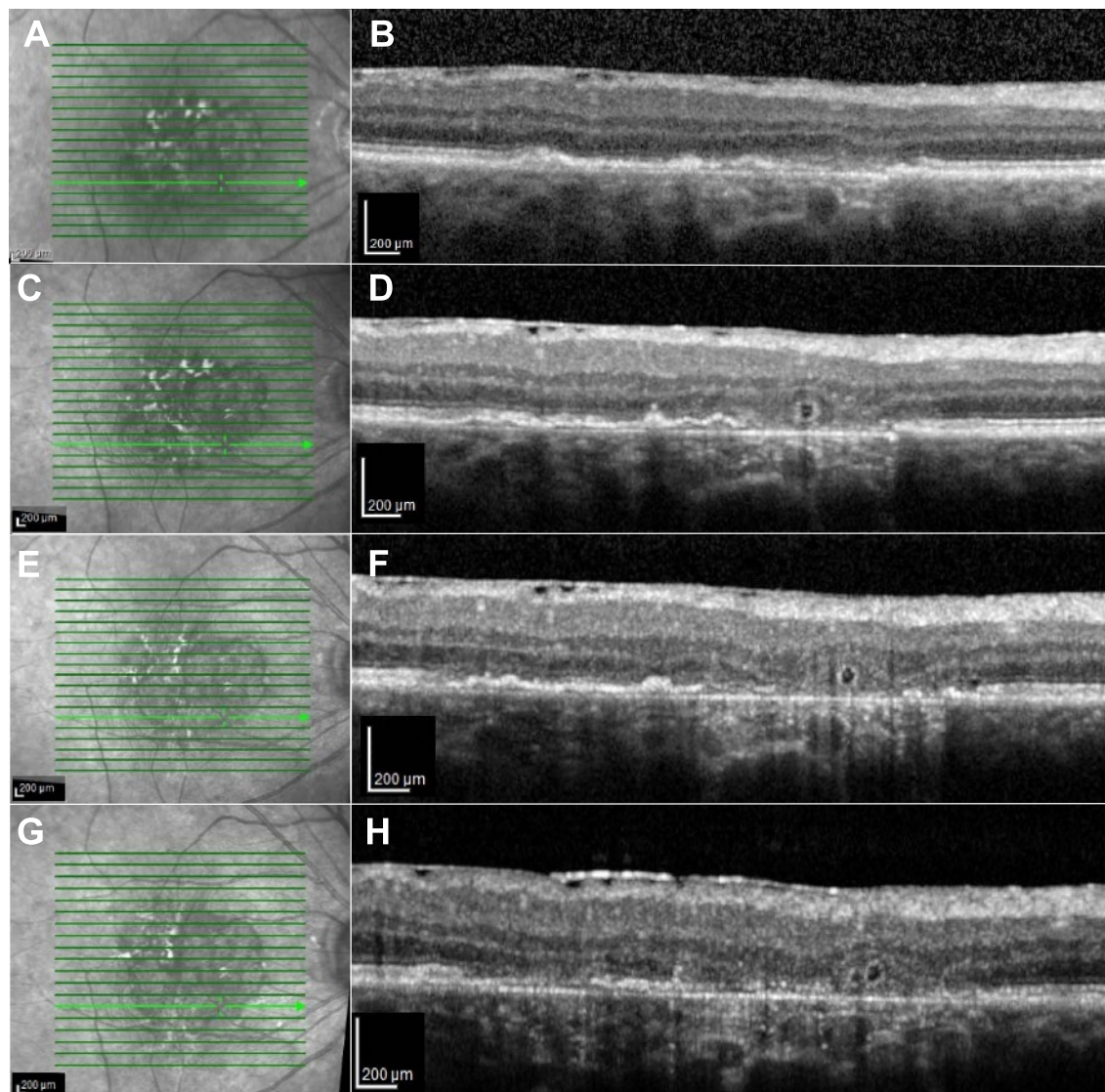


FIGURE 6.

Consecutive IR reflectance and cross-sectional SD-OCT images of an ORT over approximately 2 years in an 80-year-old subject with nonexudative AMD. (A) and (B) Onset of atrophic changes before ORT. (C) and (D) An ORT (red arrows) that has developed within the area of atrophy 6 months after (A) and (B). (E) and (F) The same ORT 1 year and 3 months after (C) and (D). Appearance of the ORT has remained relatively stable when comparing between (D) and (F). (G) and (H) The same ORT taken 1 year after (E) and (F). There seems to be a significant change in the appearance of the ORT, and it may be dividing.

present. The outer retinal tubulation was still present at the most recent measurement 2 years later. Thus, outer retinal tubulation can develop and change, but also can remain relatively stable over a period of time.

In the 18 eyes included for retinal thickness measurements, the average inner retinal thickness above outer retinal tubulation was significantly thinner than the adjacent retina (135 vs. 170 μm , $P = .004$, Student's t -test). The outer retina was significantly thicker at the outer retinal tubulations than for the adjacent retina (115 vs. 80 μm ; $P = .03$, t -test).

The adaptive optics scanning laser ophthalmoscope imaging demonstrated outer retinal tubulations to be tubular, finger-like projections that ranged in length from small projections to tubes extending across the width of atrophy (Fig. 7). These finger-like projections often extend from less abnormal retina into atrophic regions and

may divide into multiple outer retinal tubulations as confirmed by OCT b-scans. Fig. 7 (top, panels A and B) demonstrates an example of a dividing outer retinal tubulation. Additionally, the size of an individual outer retinal tubulation may vary as it extends into the atrophic region (Fig. 8).

Adaptive optics scanning laser ophthalmoscope imaging also enabled visualization of outer retinal tubulation characteristics that are not readily observed with SD-OCT. Confocal imaging of outer retinal tubulation demonstrates sparse cones found within the outer retinal tubulation (Fig. 7) as visualized by clear-cut punctate regions of hyperreflectivity with similar characteristic both in an outer retinal tubulation and in the nearby more normal cone mosaic. Multiply scattered light imaging also suggests that the structure of some cones can be visualized as part of an outer retinal tubulation (Fig. 7), with bright regions in the multiply scattered light images, generally

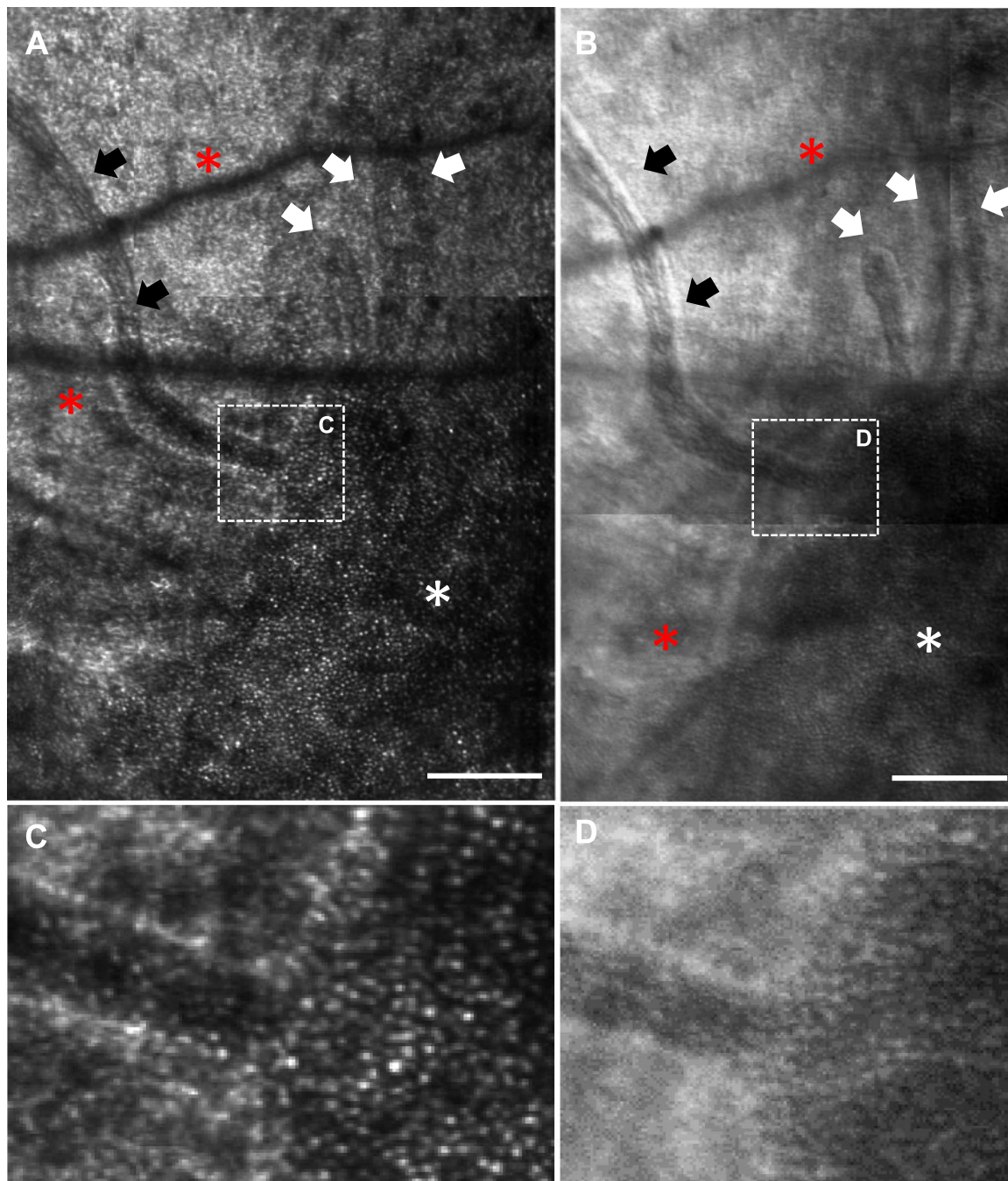


FIGURE 7.

AOSLO imaging at the border of an atrophic region of retina (red asterisk) and less abnormal retina (white asterisk) in a 56-year-old subject with rod-cone dystrophy. This region of atrophy has a long ORT bridging it (black arrows) and a several smaller ORT (white arrows) extending from the less abnormal region of retina into the atrophic region. (A) Confocal image. (B) Multiply scattered light image showing the clear borders of the ORT. (C) An enlarged region of (A) (denoted by dotted lines) showing cones extending onto the ORT. (D) An enlarged region of (B) (denoted by dotted lines) showing cones extending onto the ORT. Scale bars = 200 μm .

considered to be inner segments, associated with the bright regions in the confocal image in the adjacent retina and as part of the outer retinal tubulation (Fig. 7). Additionally, multiply scattered light imaging of the outer retinal tubulations shows a variegated appearance of structures along the wall of the outer retinal tubulation as seen in Figs. 9 and 10. Where possible, the lengths of the fine, variegated lines were measured giving values from 18 to 35 μm , with respect to the *en face* dimensions. Lastly, outer retinal tubulations have clearly

defined borders when visualized with adaptive optics scanning laser ophthalmoscope (Figs. 7 and 8) that are best visualized with multiply scattered light imaging.

DISCUSSION

These results agree with the growing consensus that outer retinal tubulations are quite common in eyes with atrophy, and

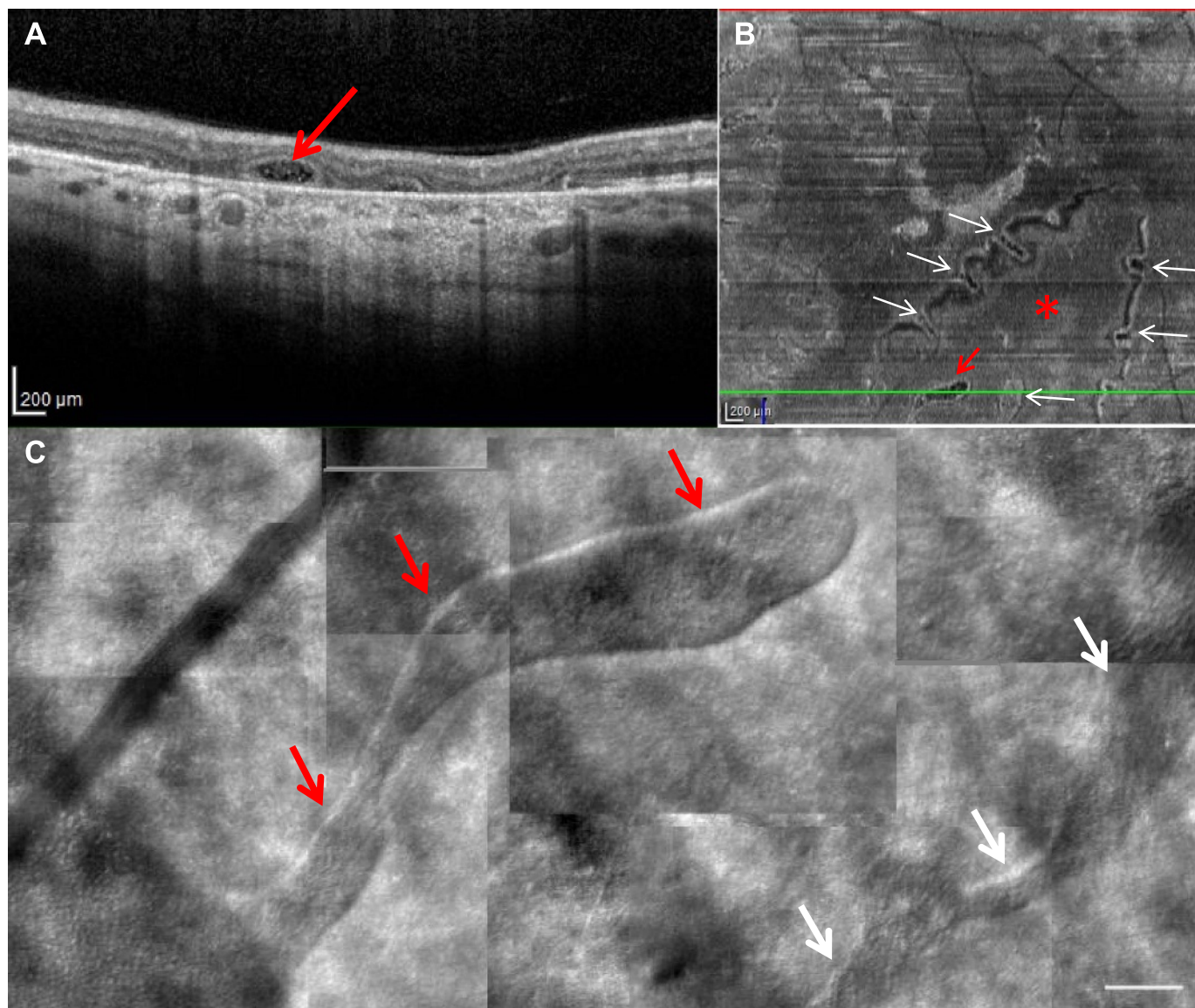


FIGURE 8.

Visualization of ORT by SD-OCT and AOSLO in a 57-year-old subject with rod-cone dystrophy. (A) Cross-sectional SD-OCT image of an ORT (red arrow) demonstrating contents within the lumen. (B) En face SD-OCT image of the same ORT (red arrow) in an area of atrophy (red asterisk). Numerous ORTs can be seen extending into this area of atrophy (white arrows). (C) The same ORT (red arrow) viewed with multiply scattered light AOSLO imaging. An additional ORT is also visible extending in this area of atrophy (white arrow). In each imaging modality, a clearly defined border can be viewed surrounding the ORT. Scale bar = 100 µm.

that different disorders lead to outer retinal tubulation formation.^{4,5} Outer retinal tubulations were found in over half of the patients within our sample with atrophy, despite the wide variety of ages. These patients had underlying etiologies ranging from age-related macular degeneration to less common entities such as thioridazine retinal toxicity. The generality of the formation of outer retinal tubulations is supported by our unique finding of outer retinal tubulation in four cases of solely peripapillary atrophy. The process of retinal damage in peripapillary atrophy is assumed to be markedly different than most of the other forms of retinal atrophy, e.g. in myopia being a result of eye growth and retinal stretching rather than primary retinal pigmented epithelium disease.²¹ Thus, we conclude that outer retinal tubulation formation is a nonspecific retinal response and emphasizes the importance of recognizing the classic SD-OCT characteristics in

the treatment and management of any number of retinal disorders. Several factors may suggest that outer retinal tubulations are even more common than our study indicates. First, our data represent a fairly short time span of disease for any given patient and outer retinal tubulations go through stages. Thus, we would expect that some of our patients with atrophy might have previously had outer retinal tubulations in locations where we did not observe them.^{12,13,22} Second, OCT b-scan spacing may cause researchers to miss some outer retinal tubulations.

The exact mechanism of the formation of outer retinal tubulation remains to be determined. However, previous studies agree that these structures appear to form after insult to the outer retinal layers, typically caused by degenerative retinal disease, in an attempt of the ellipsoid zone and external limiting membrane to reconfigure in a sort of “rolling” mechanism.^{2,4} This is supported by the morphology

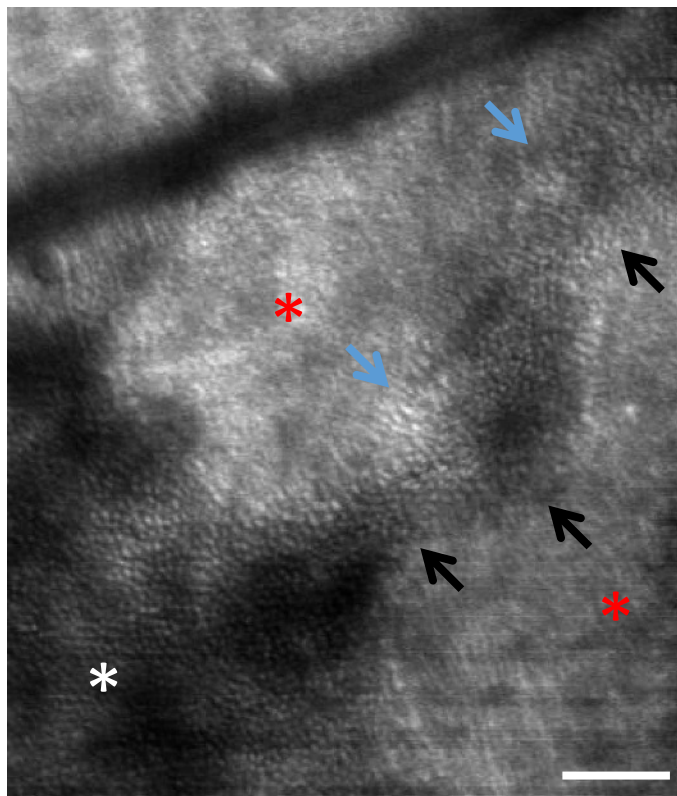


FIGURE 9.

Multiply scattered light AOSLO image of visible cones within an ORT in a 57-year-old subject with rod-cone dystrophy. Numerous cones are visible within and around the borders of the ORT (black arrow) as it bridges the junction of atrophic (red asterisk) and more normal (white asterisk) retina. Variegated structures (blue arrows) are also visualized. Scale bar = 100 μm .

of what are hypothesized to be early, or forme fruste, outer retinal tubulation.¹¹ In our SD-OCT images, most of these forme fruste outer retinal tubulations were found at the borders of areas of normal and atrophic outer retina.

It is evident that the development of outer retinal tubulation is associated with insult to the outer retinal layers. Yet, there are surviving photoreceptors within areas of atrophy, as seen on histology,^{12,13} SD-OCT,^{2–5,8,9,22–24} and now adaptive optics scanning laser ophthalmoscope. An intriguing possibility is that this photoreceptor arrangement provides a survival benefit for the photoreceptors that are located over regions of diseased or missing retinal pigmented epithelium. Outer retinal tubulations form whether the retinal pigmented epithelium is missing because of primary disease, as in age-related macular degeneration, or the retinal pigmented epithelium is separated from the overlying retina, as in peripapillary atrophy.²¹ With the loss of choriocapillaris seen in geographic atrophy, this curling of the photoreceptors may provide a nutritional survival by either acting as conduit or increasing proximity to overlying retinal vasculature and neighboring Muller cells as indicated by the decrease in inner retinal thickness above outer retinal tubulations reported here. Additional investigations into the inner and outer retinal thickness differences will be needed to fully understand this relation.

Adaptive optics scanning laser ophthalmoscope provides further insight of the *in vivo* characteristics of outer retinal tubulation and outer retinal tubulation formation at the cellular level. As noted

above, adaptive optics scanning laser ophthalmoscope confirms the finding of SD-OCT *en face* imaging of the branching nature of the outer retinal tubulations that tend to extend from regions of less abnormal to atrophic regions of retina. Only one outer retinal tubulation was found in our *en face* imaging that was completely enclosed within an area of atrophy (Fig. 5). Cones were clearly visible in some outer retinal tubulations (Figs. 7, 9, and 10) despite their location in an area of atrophy. Although these images demonstrate that cones are present, they can have an elongated structure that likely arises from the orientation in the outer retinal tubulation. Although they can be imaged *in vivo*, their role in visual function cannot be determined from adaptive optics scanning laser ophthalmoscope imaging alone. However, this finding is consistent with histological analysis that outer retinal tubulations contain cone nuclei with inner and outer segment components oriented radially into the lumen of the outer retinal tubulations.¹¹ This histological analysis also demonstrated varying stages of cone degeneration within the outer retinal tubulations ranging from nascent to end-stage phases of the outer retinal tubulations.¹¹ A range of appearance of outer retinal tubulations consistent with histology can be seen in some of the adaptive optics scanning laser ophthalmoscope images (comparing Figs. 7–9).¹¹

Additionally, we show that multiply scattered light with an adaptive optics scanning laser ophthalmoscope reveals variegated structures along the anterior surface of the outer retinal tubulation. The measured lengths appear to be longer than what has been reported for degenerating inner segments, but may be consistent with the

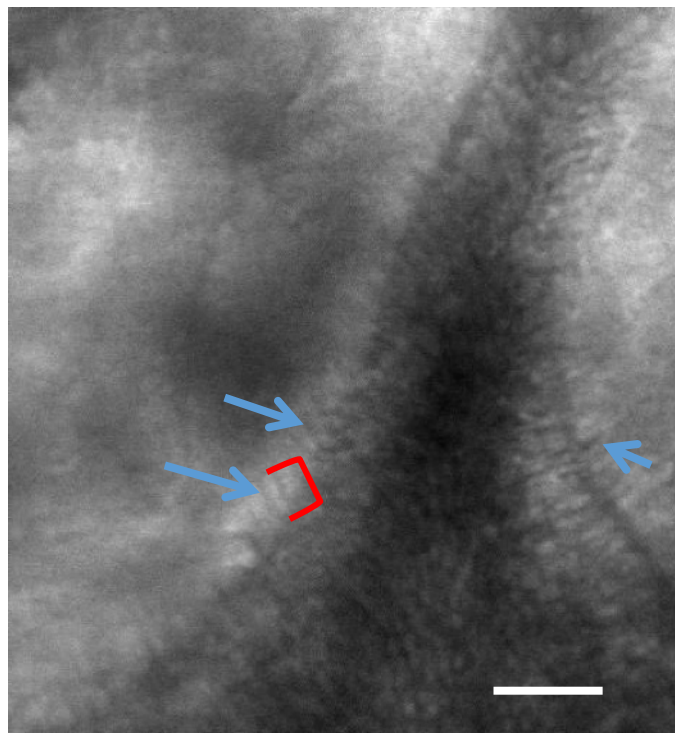


FIGURE 10.

Multiply scattered light AOSLO image of variegated structures along ORT wall. Variegated structures (blue arrows) are visible that appear to line the walls of ORTs. One of these structures has been bracketed in red for better individual visualization. These structures range in size from 18 to 35 μm . Scale bar = 50 μm . SD-OCT images of this ORT can be viewed in Fig. 4A (dashed lines) and 4B.

length of photoreceptor inner segments and Muller cell complex,¹² thus suggesting an inward rolling of the photoreceptors in the formation of the outer retinal tubulation and opens the possibility for future studies to better follow this process *in vivo*.

Furthermore, distinct borders of the outer retinal tubulations were observed in all patients, which are in agreement with the hyperreflective borders observed with SD-OCT. From histological analysis, a major component of this border is the external limiting membrane and mitochondria.^{11,13} This border persists in outer retinal tubulation regardless of the stage of cone degeneration.¹¹

Although adaptive optics scanning laser ophthalmoscope imaging suggests that there are radially oriented cones associated with outer retinal tubulations, other contents cannot be distinguished.¹¹ As we have found cones within the outer retinal tubulations throughout the atrophic retinal regions, we are in agreement with previous studies that outer retinal tubulation is likely a survival mechanism of the outer retina. Thus, outer retinal tubulations may provide a link between viable and atrophic tissue. Further supporting this hypothesis is the fact that outer retinal tubulation presence has been associated with decreased progression of geographic atrophy when compared with geographic atrophy without outer retinal tubulations, leading to a conclusion that this link may act as a conduit between surviving retinal pigmented epithelium and areas of atrophy.¹¹ Another possible explanation may be the change in proximity to the inner retinal circulation, which occurs in the presence of outer retinal tubulation as suggested from our results.

In conclusion, outer retinal tubulation is a common finding seen in a variety of retinal degenerations, which may serve as a survival mechanism for photoreceptors within areas that lack proper nutritional supply secondary to outer retinal damage and loss of underlying choriocapillaris. They are encountered frequently in clinical settings that utilize SD-OCT and should be differentiated from intraretinal fluid to avoid unnecessary treatment.² Recent histological analysis has provided a great deal of insight into the contents of outer retinal tubulation and photoreceptor degeneration in age-related macular degeneration,¹¹ and adaptive optics scanning laser ophthalmoscope imaging provides *in vivo* details of the outer retinal tubulations at resolutions that exceed commercially available clinical instrumentation. The ability to identify surviving cones in regions of atrophy may be a biomarker for potential therapeutic interventions.

ACKNOWLEDGMENTS

The authors thank Alberto de Castro, Ting Luo, and Lucie Sawides for aid in patient imaging.

This work was supported by NIH Grants R01 EY04395 and Foundation Fighting Blindness Grant TA-CL-0613-0617-IND (Burns) and Core Grant P30EY019008 and NIH Grant R01 EY007624 (Elsner). The sponsor or funding organization had no role in the design or conduct of this research. Disclosures: S.A.B., fees for consulting for Nidek and Boston Micromachines; A.E.E., ownership for AEON Imaging.

The authors acknowledge part of this study was presented as a poster "Outer Retinal Tubulation Observed with SD-OCT and AOSLO" at the 2014 ARVO meeting, May 4–8, 2014 in Orlando, FL and a paper "Comparison of Inner Retinal Thickness Over and Adjacent to Outer Retinal Tubulation" presented at the American Academy of Optometry meeting in Denver, CO, November 13, 2014.

Received March 3, 2016; accepted September 29, 2016.

REFERENCES

- Bhutto I, Luty G. Understanding age-related macular degeneration (AMD): relationships between the photoreceptor/retinal pigment epithelium/Bruch's membrane/choriocapillaris complex. *Mol Aspects Med* 2012;33:295–317.
- Zweifel SA, Engelbert M, Laud K, et al. Outer retinal tubulation a novel optical coherence tomography finding. *Arch Ophthalmol* 2009;127:1596–602.
- Dolz-Marco R, Gallego-Pinazo R, Pinazo-Duran MD, et al. Outer retinal tubulation analysis in cases of macular dystrophy. *Arch Soc Esp Oftalmol* 2013;88:161–2.
- Goldberg NR, Greenberg JP, Laud K, et al. Outer retinal tubulation in degenerative retinal disorders. *Retina* 2013;33:1871–6.
- Iriyama A, Aihara Y, Yanagi Y. Outer retinal tubulation in inherited retinal degenerative disease. *Retina* 2013;33:1462–5.
- Morgan JIW, Han G, Klinman E, et al. High-resolution adaptive optics retinal imaging of cellular structure in choroideremia. *Invest Ophthalmol Vis Sci* 2014;55:6381–97.
- Wolff B, Maftouhi MQ, Mateo-Montoya A, et al. Outer retinal cysts in age-related macular degeneration. *Acta Ophthalmol* 2011;89:e496–9.
- Hariri A, Nittala MG, Sadda SR. Outer retinal tubulation as a predictor of the enlargement amount of geographic atrophy in age-related macular degeneration. *Ophthalmology* 2015;122:407–13.
- Moussa K, Lee JY, Stinnett SS, et al. Spectral domain optical coherence tomography-determined morphologic predictors of age-related macular degeneration-associated geographic atrophy progression. *Retina* 2013;33:1590–9.
- Curcio CA, Medeiros NE, Millican CL. Photoreceptor loss in age-related macular degeneration. *Invest Ophthalmol Vis Sci* 1996;37:1236–49.
- Schaal KB, Freund KB, Litts KM, et al. Outer retinal tubulation in advanced age-related macular degeneration: optical coherence tomographic findings correspond to histology. *Retina* 2015;35:1339–50.
- Litts KM, Messinger JD, Freund KB, et al. Inner segment remodeling and mitochondrial translocation in cone photoreceptors in age-related macular degeneration with outer retinal tubulation. *Invest Ophthalmol Vis Sci* 2015;56:2243–53.
- Litts KM, Messinger JD, Dellatorre K, et al. Clinicopathological correlation of outer retinal tubulation in age-related macular degeneration. *JAMA Ophthalmol* 2015;133:609–12.
- King BJ, Elsner AE, Papay JA, et al. Comparison of inner retinal thickness over and adjacent to outer retinal tubulation. *Optom Vis Sci* 2014;91:E-abstract 140044.
- Zayit-Soudry S, Duncan JL, Syed R, et al. Cone structure imaged with adaptive optics scanning laser ophthalmoscopy in eyes with nonneovascular age-related macular degeneration. *Invest Ophthalmol Vis Sci* 2013;54:7498–509.
- Ferguson RD, Zhong Z, Hammer DX, et al. Adaptive optics scanning laser ophthalmoscope with integrated wide-field retinal imaging and tracking. *J Opt Soc Am (A)* 2010;27:A265–77.
- Burns SA, Elsner AE, Chui TY, et al. In vivo adaptive optics microvascular imaging in diabetic patients without clinically severe diabetic retinopathy. *Biomed Opt Express* 2014;5:961–74.
- Elsner A, Miura M, Burns S, et al. Multiply scattered light tomography and confocal imaging: detecting neovascularization in age-related macular degeneration. *Opt Express* 2000;7:95–106.
- Chui TY, Vannasdale DA, Burns SA. The use of forward scatter to improve retinal vascular imaging with an adaptive optics scanning laser ophthalmoscope. *Biomed Opt Express* 2012;3:2537–49.

20. Huang G, Zhong ZY, Zou WY, et al. Lucky averaging: quality improvement of adaptive optics scanning laser ophthalmoscope images. *Opt Lett* 2011;36:3786–8.
21. Nakazawa M, Kurotaki J, Ruike H. Long-term findings in peripapillary crescent formation in eyes with mild or moderate myopia. *Acta Ophthalmol* 2008;86:626–9.
22. Jung JJ, Freund KB. Long-term follow-up of outer retinal tubulation documented by eye-tracked and en face spectral-domain optical coherence tomography. *Arch Ophthalmol* 2012;130:1618–9.
23. Lee JY, Folgar FA, Maguire MG, et al. Outer retinal tubulation in the comparison of age-related macular degeneration treatments trials (CATT). *Ophthalmology* 2014;121:2423–31.
24. Wolff B, Matet A, Vasseur V, et al. En face OCT imaging for the diagnosis of outer retinal tubulations in age-related macular degeneration. *J Ophthalmol* 2012;2012:542417.

Brett J. King

*School of Optometry
Indiana University Bloomington
800 E Atwater Ave
Bloomington, IN 47405-3635
e-mail: kingbrj@indiana.edu*